Polym. Bull. (2009) 62:405–419
DOI 10.1007/s00289-008-0019-6

ORIGINAL PAPER

Nucleating agent induced impact fracture behavior change in PP/POE blend

Hongwei Bai · Yong Wang · Bo Song · Ximei Fan · Zuowan Zhou · Yanli Li

Received: 12 August 2008 / Revised: 31 October 2008 / Accepted: 30 November 2008 /
Published online: 11 December 2008

Abstract This work was focused on the impact fracture behavior of polypropylene/ethylene-octene copolymer (PP/POE) blends with and without nucleating agent (NA). The crystallization morphologies of injection-molded-bar were analyzed by polarization optical microscope and the impact-fractured surface morphologies were characterized carefully through scanning electronic microscope. Our results show that the addition of 0.2 wt% α/or β-NA induces the great decrease of spherulites diameters companioned with the dramatically enhancement of PP/POE blend toughness. Virgin PP shows the typical brittle-fractured characteristic during the whole fracture process. PP/POE shows the less-ductile fracture feature with multiple-craze formation. The addition of NA into PP/POE blend changes the fractured surface feature from predominantly multiple-craze to predominantly shear yielding or shear yielding involving materials cavitations and second-crack re-initiation, respectively, indicating the change from brittle-like fracture mode to ductile fracture mode. The transformation of $\beta \rightarrow \alpha$ during the impact process for β-NA nucleated samples has been observed; however, such transformation is suppressed by the presence of POE.

Keywords PP/POE blend · Nucleating agent · Impact fracture behavior

Introduction

Polypropylene (PP) is an important semicrystalline polymer that has been widely used in many fields due to its excellent properties. However, its serious brittle response, especially at low temperature or/and high strain rate, limits its application

H. Bai · Y. Wang (✉) · B. Song · X. Fan · Z. Zhou · Y. Li
Key Laboratory of Advanced Technologies of Materials (Ministry of Education),
School of Materials Science and Engineering, Southwest Jiaotong University,
610031 Chengdu, China
e-mail: yongwang1976@163.com

as an engineering material. To improve the unfavorable toughness, various elastomers [1–5] were developed to blend with PP. During the last decades, almost studies about elastomer toughened polymer have been done based on the content and properties of elastomer [6–8], particle size and spatial distribution of elastomer [9–11], elastomer particles deformation [12, 13], interfacial adhesion between elastomer particles and matrix [14] and so on. Simultaneously, several toughening mechanisms have also been proposed to explain the improvement of toughness, such as multiple crazing [15], shear yielding [16], cavitations [17], and percolation [18].

Besides the effect of elastomer particles, the matrix properties are also those of the key factors which determine the toughness improvement of PP/elastomer blends. Van der Wal [19] has revealed that the brittle–ductile temperature (T_{bd}) of PP/EPDM blends shifts to higher temperatures with increasing crystallinity of PP or decreasing molecular weight of PP. Jiang's work has shown that the product of yield stress and yield strain of matrix is a key factor that determines the brittle–ductile transition (BDT) of elastomer toughened PP blends [20]. Recent work about the toughening effect of elastomer on PP is focused on controlling the spherulites diameters or crystalline structure (typically α-phase and β-phase) of PP through addition of NA [21–24] For example, high impact strength has been achieved by addition of a few amounts of β-NA into elastomer toughened PP blends [21]. For α-NA modified PP/elastomer blends, at least two different phenomena have been observed for impact strength. One is the addition of a few amounts of α-NA into elastomer toughened PP results in a great enhancement of blends toughness [22, 23], and the other is that the presence of α-NA produces an increase in storage and flexural modulus at the expense of a slight decrease in impact strength compared with the binary blends [24].

So far, the toughening mechanisms of elastomer toughened PP blends with NA are fragmented and less examined. Almost work is simply analyzing the effects of NA on crystalline structure and mechanical properties of PP/elastomer blends, and is absent in toughening mechanism, especially in the understanding of the fracture process. In the present work, our attention is paid to the impact fracture behaviors of PP/elastomer blend with and without NA. Two kinds of NAs, i.e., α-NA 1,3:2,4-bis (3,4-dimethylbenzylidene) sorbitol (DMDBS, Millad 3988) or β-NA aryl amides compounds (TMB-5), were used to modify PP/POE blends. In the former system, α-PP is the exclusively crystalline structure, and in this condition, the fracture behavior is analyzed based on the decrease of spherulites diameters. In the latter system, β-PP is the main crystalline structure, and fracture behavior of the blends is mainly influenced not only by the special supermolecular structure of β-phase but also by the decrease of spherulites diameters and the transformation from β-PP to α-PP provoked during the impact process.

Experimental

Materials

PP (F401) with a melt flow rate (MFR) of 2.5 g/10 min (230 °C/2.16 kg) was obtained from Langang Petrochemical Co, Ltd, Lanzhou, China. POE (EXACT

5371) with a MFR of 11.0 g/10 min (190 °C/2.16 kg, ASTMD-123) was obtained from ExxonMobil Chemical Company, USA. The α-NA 1,3:2,4-bis(3,4-dimethylbenzylidene) sorbitol (DMDBS, Millad 3988) was supplied by Milliken Chemical, Belgium, and the β-NA aryl amides compound (TMB-5) was provided by Fine Chemicals Department of Shanxi Provincial Institute of Chemical Industry, China.

Sample preparation

A master batch of 5 wt% NA in PP was first prepared through melt blending of NA and PP, and then a certain amount of master batch was melt blended with PP and POE to obtain the corresponding ternary samples. In this work, NA (DMDBS or TMB) content was maintained at 0.2 wt% of PP in weight fraction and POE content was 15 wt%. Binary systems of PP/α-NA (0.2 wt%), PP/β-NA (0.2 wt%) and PP/POE (85/15) were also prepared. The melt blending of such blends was conducted on a twin-screw extruder (TSSJ-25, China) with a screw speed of 120 r/min and temperatures of 150–215 °C from hopper to die. After making droplets, the pellets were injection-molded and the standard specimens for impact test were prepared using an injection-molding machine (K-TEC 40, Germany) with melt temperatures of 190–215 °C and mould temperature of 25 °C.

Notched Izod impact strength

Notched Izod impact strength was measured using an impact tester (XC-22Z, China) according to ISO179-1982. For each sample, the average value reported was derived from at least five test bars. All the measurements were carried out at room temperature (23 °C).

Crystallization behavior and crystalline morphology

Differential scanning calorimetry (DSC, Netzsch STA 449C Jupiter, Germany) was used to investigate the crystallization and melting behaviors of the blends. The weight of each sample was about 8 mg. Firstly, the sample was heated from 30 to 200 °C at the heating rate of 10 °C/min and maintained at 200 °C for 5 min to erase the thermal history; secondly, the sample was cooled down to 30 °C at the cooling rate of 10 °C/min. The measurement was carried out in helium atmosphere. A microtome (RM2245, Leica) was firstly used to cut a slice with a thickness of about 15 μm from the injection-molded bar perpendicularly to the flow direction. The slice was then sandwiched between two glass slides and placed on a stage of polarization optical microscope (POM, XPN-203, China) and the crystalline morphology of the sample was taken images via a digital camera.

Fractography

The impact-fractured surfaces were characterized by using a Fei Quanta 200 environmental scanning electronic microscope (ESEM, America) with an accelerating voltage of 20 kV after coating with a gold layer. Here, each macroscopic

fractured surface was divided into two zones, i.e., initiation zone and propagation zone. For all of the PP/POE blends with and without NA, the comparison of fracture behaviors between the corresponding zones was chosen almost at the same region.

Crystalline structure transformation during the impact process

Wide angle X-ray diffraction (WAXD, Panalytical X'pert PRO diffractometer with Ni-filtered CuKα radiation, Holland) and DSC were used to characterize the possible crystalline structure transformation during the impact process. For WAXD measurement, the cross section of the injection-molded bar was first measured and the results indicate the crystalline structure before impact process. Then, the same bar was impact fractured and the impact-fractured surface was measured again and the results indicate the crystalline structure after impact process. The β-PP fraction (K_β) in the samples was calculated from WAXD diffractograms according to the following relation [25]:

$$K_\beta = I^\beta_{300}/(I^\alpha_{110} + I^\alpha_{040} + I^\alpha_{130} + I^\beta_{300}) \quad (1)$$

where $I^\alpha_{110}, I^\alpha_{040}$ and I^α_{130} are the integral intensities of the (110), (040) and (130) reflections of the α-phase, respectively, and I^β_{300} is the integral intensity of (300) reflection of β-PP. For DSC measurement, the samples about 3 mg were cut carefully from the cross-section of a bar (before impact) and the stress whitening zone of the impact-fractured surface (after impact), respectively. Then, the sample was heated from 30 to 200 °C at the heating rate of 10 °C/min in the nitrogen atmosphere.

Results and discussion

Crystallization behavior and crystalline morphology

The crystallization behaviors of PP/POE blend with and without NA were investigated by DSC and the crystallization parameters (typically crystallization temperatures T_c) are summarized in Table 1. The results of PP nucleated by individual NA are also shown in the table. Apparently, PP/POE blend shows higher T_c compared with virgin PP, indicating a weak nucleation effect of POE for PP

Table 1 Crystallization temperature (T_c) and impact toughness of virgin PP, PP/NA and PP/POE/NA blends

Sample	T_c (°C)	Impact strength (kJ/m^2)
PP	109.1	4.2
PP/α-NA	125.7	4.3
PP/β-NA	121.2	6.1
PP/POE (85/15)	113.5	14.7
PP/POE/α-NA (85/15/0.2)	125.7	41.3
PP/POE/β-NA (85/15/0.2)	123.3	59.5

crystallization. The T_c of PP/POE/NA sample is much higher than that of PP/POE blend and very close to the T_c of PP/NA, which means that the nucleation effect of NA in PP/POE blend is very apparent and the crystallization behavior of PP is strongly governed by NA rather than by POE.

Generally, the significant morphological feature of β-PP is a stacked, parallel arrangement of bundles of lamellae, whereas so-called "cross-hatched" arrangement of the lamellar crystal for α-PP [26]. Then, α-PP and β-PP can be easily distinguished by the observation with POM based on their very different optical properties. Figure 1 shows the typical crystallization morphologies in the core regions of PP, PP/POE and PP/POE/NA injection-molded bars. Virgin PP shows the typical α-spherulites and the average diameter of PP spherulites is about 50–80 μm (indicated by the circles in Fig. 1a). Smaller dominant α-spherulites (about 20–30 μm) are observed for PP/POE blend, further proving the weak nucleation effect of POE particles as described above. For NA nucleated PP/POE blend, the spherulites decrease greatly with very homogeneous dispersion. At higher magnification, the spherulites diameters are calculated as 1–5 and 5–15 μm for DMDBS and TMB-5 nucleated blends, respectively. This indicates the excellent nucleation effect of NA on PP crystallization by dramatically increasing the nucleation density and significantly reducing the spherulites diameters. Importantly, β form spherulites distinctly different from the α-spherulites exists exclusively in

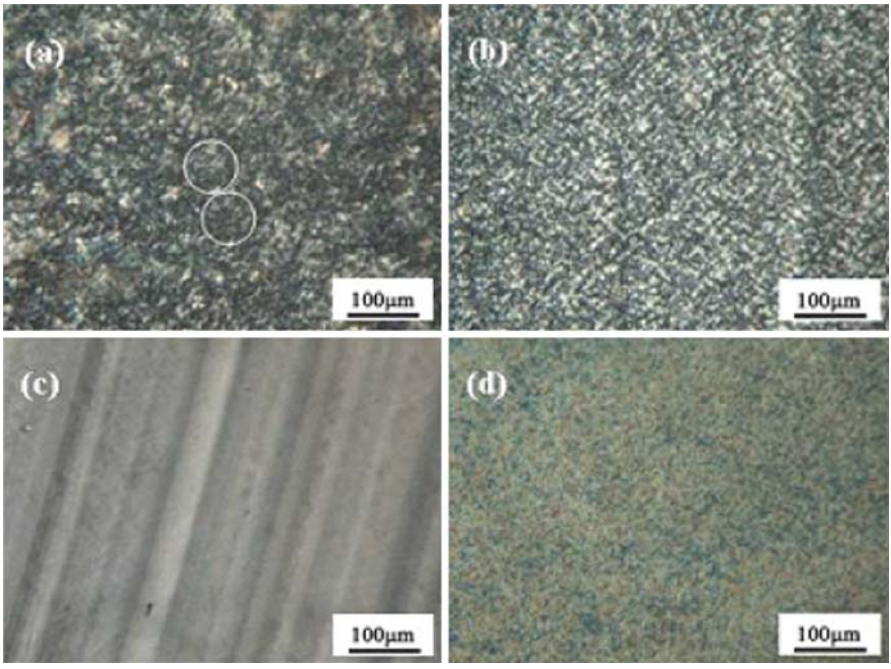

Fig. 1 Polarized optical micrographs of virgin PP and nucleated PP/POE blends sectioned from the core regions of injection-molded bars: **a** Virgin PP, **b** PP/POE (85/15), **c** PP/POE/α-NA (85/15/0.2), and **d** PP/POE/β-NA (85/15/0.2)

β-NA nucleated blends (Fig. 1d), which can enhance energy dissipating during deformation.

Impact toughness

The notched Izod impact strength of samples is also listed in Table 1. NA nucleated PP shows a slightly increase of impact strength compared with virgin PP. The impact strength of PP/POE blend is 14.7 kJ/m^2, higher than that of virgin PP, suggesting an apparent toughening effect of POE on PP. Interestingly, the presence of NA in PP/POE blend induces a dramatically increase of impact strength compared with PP/POE blend. The impact strength is increased up to 41.3 and 59.5 kJ/m^2 for PP/POE/α-NA and PP/POE/β-NA, respectively. Furthermore, PP/POE/β-NA presents higher impact strength compared with PP/POE/α-NA due to the formation of large amounts of β-PP induced by TMB-5.

Impact fracture behavior analysis based on fractograph

To gain further insight in understanding the role of NA on PP/POE blend toughness, it is very important to analyze the fracture process of the samples. In this work, the fracture process will be estimated based on the analysis of impact-fractured surface morphologies governed by the initiation and propagation of crack.

Impact fracture behavior of virgin PP

Figure 2 shows the impact-fractured surface morphologies of virgin PP and these morphologies clearly indicate a typical brittle fracture mode. Macroscopically, the whole fractured surface (at low magnification, seen in Fig. 2a) is very flat and smooth without any considerable shear yielding or plastic deformation. The fractured surface can be differentiated as two different zones along the impact fracture direction, i.e., initiation zone and propagation zone. Both the initiation and propagation zones can be further subclassified. For initiation zone, it includes zones A and B. Zone A is in the core region of injection-molded bar and zone B is related

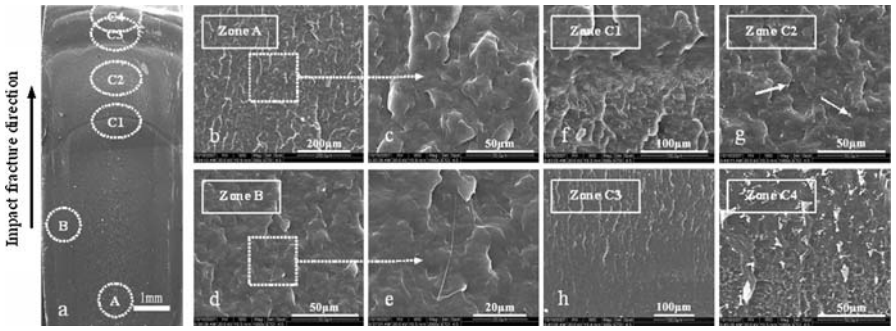

Fig. 2 SEM pictures of impact fracture surface of pure PP; the crack propagation direction is indicated by the *arrow*

to the edge of bar. At higher magnification (Fig. 2b and c), zone A displays a craze-like brittle morphology with "patch" appearance and Zone B with more "patch" and some microfibrils (Fig. 2d and e). These microfibrils maybe related to the orientation texture in the edge of the molded-bar.

After the initiation of crack, the fracture faces the rapid crack propagation process. The rapid crack propagation zone presents the similar fracture characteristics compared with the initiation zone (not shown here). However, at the later stage of crack propagation, the fractured surface can be further divided into four zones. Zone C1 (Fig. 2f) is a small zone with a parabolic ridge or a thin curved band. Normally, such appearance is related to the stick-slip type propagation during the scratch deformation in polymeric materials. Misra [27, 28] believes that the stick-slip or stop-go propagation, associated with the dynamic crack propagation effects, occurs when the crack speed is below the critical value—the crack stops or arrests (sticks). If the stress increases again, the crack re-initiates and propagates again (slips). During the stick-slip stage, local plastic deformation occurs around the stopped crack involving some stable growth.

After the stick-slip process in zone C1, a new crack re-initiates and propagates unstably until it is arrested again in zone C3. Zone C2 (Fig. 2g) presents the similar appearance compared with the early stage of the crack propagation, although some tiny yielding sheets (indicated by the arrows) are observed in this zone. Subsequently, the crack propagation suffers another stop-go propagation process. It should be mentioned that the area of zone C3 (Fig. 2h) is much larger than that of zone C1, implying the crack propagation rate in zone C2 becomes slower compared to that in the early stage of first crack propagation stage, and more stress is needed to re-initiate the crack again. In zone C4 (Fig. 2i), the last stage of crack propagation, a vein-type features involving tearing of the material are observed, indicating the severe local plastic deformation. However, the area of such zone is very small compared with the whole fracture process, and it has no significant contribution to the toughness of PP.

Impact fracture behavior of PP/POE binary blend

Figure 3 shows the impact-fractured surface morphologies of PP/POE blend. As expected, the overall fracture surface shows less-ductile feature with multiple-craze formation macroscopically (Fig. 3a). In the initiation zone (zone A, Fig. 3b, c) and the early stage propagation zone, including the zone related to the edge of bar (zone B, Fig. 3d, e), the blend presents the similar fracture feature compared with virgin PP, namely, a "patch" appearance. However, the size of each "patch" in the blend is much larger than that of in virgin PP, and some inconspicuous plastic deformation markings exists in the "patch", especially in the zone B, implying less-ductile behavior of the blend.

Remarkably, a distinct difference in the fracture surface of the blend from that of virgin PP is that the stick-slip stage moves further away from the root of notch and becomes inconspicuous (zone C1, Fig. 3f). After the stop–go propagation process, in zone C2 (Fig. 3g), some striations or fibrils, parallel to the local direction of crack growth but perpendicular to the impact fracture direction, can be observed clearly.

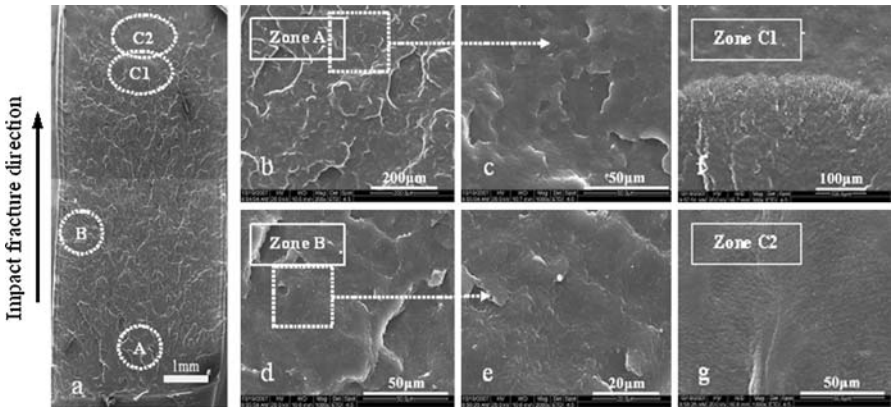

Fig. 3 SEM pictures of impact fracture surface of PP/POE (85/15); the crack propagation direction is indicated by the *arrow*

Previous studies have demonstrated that these striations can effectively depress the propagation of the local craze and then improve the dissipation of external impact energy by provoking the local plastic deformation of matrix [29, 30]. That's the reason why POE toughened PP shows much higher impact strength than virgin PP.

Impact fracture behavior of PP/POE with NA

Here, we first describe the fracture characteristics of DMDBS nucleated PP/POE blend. In PP/POE/α-NA bar, α-PP is the exclusively crystalline structure. So, the great improvement of toughness described above is mainly ascribed to the sharp decrease of spherulites diameters and their homogeneous dispersion [22, 23]. Compared with PP/POE bar, the overall fractured surface of PP/POE/α-NA bar is characterized by a significant ductile behavior macroscopically (Fig. 4a). A less-ductile feature with "patch" appearance accompanied with many yielding sheets is observed in the initiation zone (zone A, Fig. 4b, c), indicating the large energy

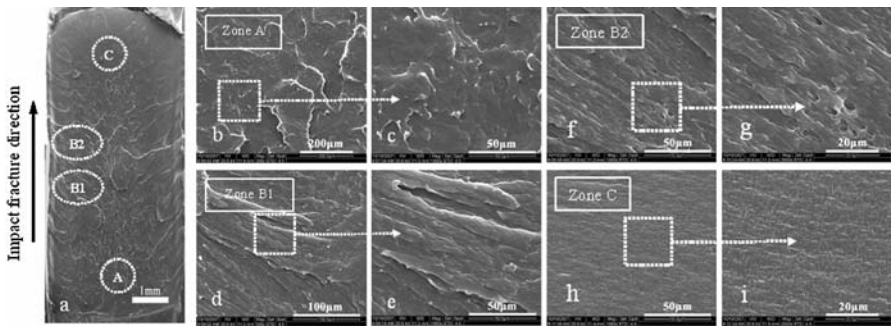

Fig. 4 SEM pictures of impact fracture surface of PP/POE/α-NA (85/15/0.2); the crack propagation direction is indicated by the *arrow*

absorption during the crack initiation process. Furthermore, one should notice that the area of zone A in PP/POE/α-NA is much smaller than that in virgin PP or PP/POE. Along the impact fracture direction, the surface morphologies associated with the crack propagation in the edge of bar can be further classified into two zones. Zone B1 shows a large plastic deformation of materials (Fig. 4d, e), and zone B2 presents not only the severe plastic deformation in a large area but also the formation of many tiny cavities (Fig. 4f, g). This may be the result of the plastic glide in the lamellae in large region. Considering the large area of zone B in the whole fractured surface and the considerable plastic deformation in such zone, it can be deduced that zone B presents the essential contribution to the great improvement of toughness of PP/POE/α-NA. At the later stage of crack propagation, zone C (Fig. 4h, i), many and very small plastic deformation sheets are visible too. Above all, the fracture of PP/POE/α-NA sample involves the severe plastic deformation process, and the sample shows very good impact toughness (41.3 kJ/m^2). In other words, the addition of a few amounts of DMDBS into PP/POE blend increases the degree of plastic deformation during the fracture process.

For TMB-5 nucleated PP/POE blend, the severe shear yielding deformation involving largely tearing of PP matrix spreads all over the fractured surface (Fig. 5a). The initiation zone can be further classified into two zones: ductile-like zone (zone A1) and ductile zone with small vein-type features (zone A2). Besides the feature of "patch" appearance accompanied with many yielding sheets that observed in the same zone of PP/POE/α-NA, zone A1 of PP/POE/β-NA also involves the material tearing parallel to the crack propagation direction and the formation of elongated voids (Fig. 5b). Furthermore, some tiny second-cracks are provoked perpendicular to the elongated voids (Fig. 5c). It is most likely that the plastic glide in the lamellae is accompanied with the tearing of amorphous zone of β-PP. Very close to the initiation zone A1, zone A2 presents not only the observed elongated voids in zone A1 but also amounts of toughening cavities formation (Fig. 5d, e). The fracture features in zone A1 and zone A2 clearly indicate that shear yielding or plastic deformation associated with the large energy absorption is provoked at the beginning of the fracture process of PP/POE/β-NA. Similarly, the crack propagation in the edge of bar can be further classified into two zones. Zone B1 is close to the initiation zone, besides the formation of plastic deformation in large area, many second-cracks are provoked perpendicular to the crack propagation or plastic deformation direction (Fig. 5f, g). This morphology is also observed in the initiation zone. However, the degree of plastic deformation and the density of second-cracks are much higher than those observed in the initiation zone. Zone B2 (Fig. 5h, f) presents more severe plastic deformation or broader shear yielding bands accompanied with largely striations or fibrillations compared with zone B1. From Fig. 5a one can see that the area of zone B is determinable in the whole fractured surface, so, it can be deduced that the plastic deformation and second-cracks formation is the main reason for the great improvement of PP/POE/β-NA toughness. A relative smooth fractured surface is also observed in zone C, involving the stress-stop-go process and the crack re-initiation again. However, different from PP/POE/α-NA in the same zone, PP/POE/β-NA bar shows plentiful striations formation perpendicular to the crack propagation direction (Fig. 5j, k). Again, the

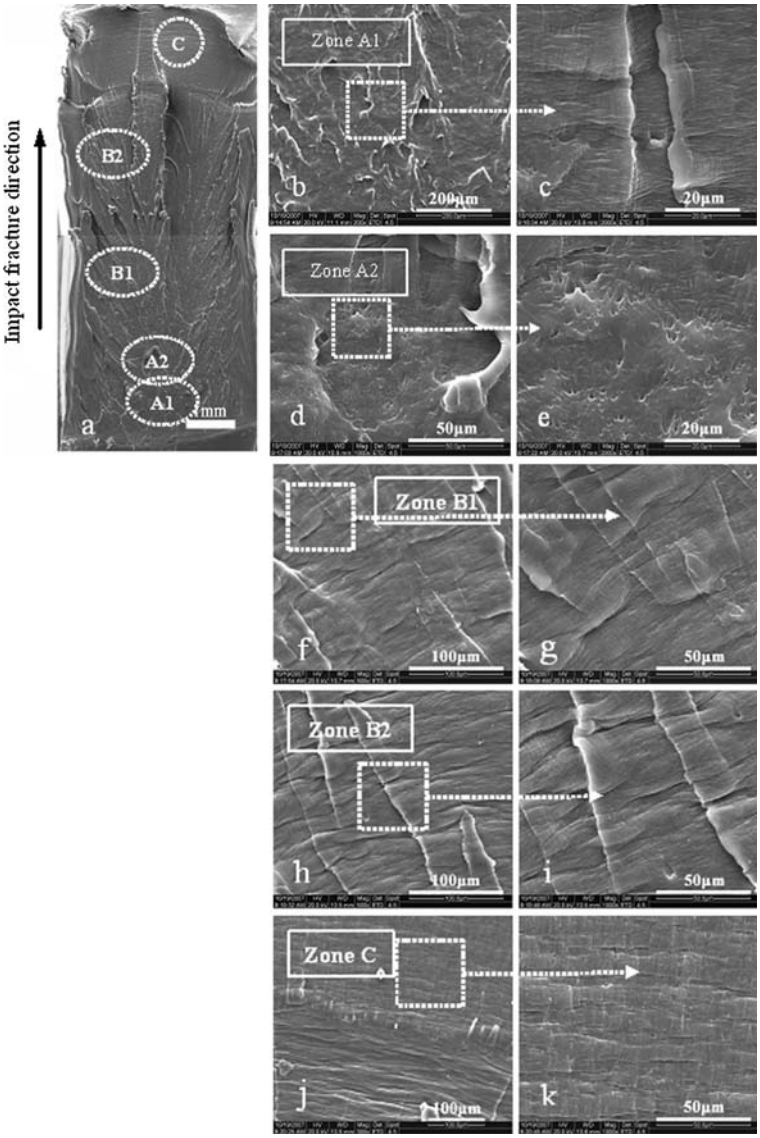

Fig. 5 SEM pictures of impact fracture surface of PP/POE/β-NA (85/15/0.2); the crack propagation direction is indicated by the *arrow*

spacing between the striations is larger than that of PP/POE/α-NA bar in the same zone.

Based on the above relative comparison of the fracture surface morphologies among virgin PP, PP/POE and PP/POE/NA, the appearance of the fractured surface can be sketched approximately in Fig. 6. It is clear that the addition of NA into PP/POE blend alters the fracture surface characteristic from predominantly multiple craze (Fig. 6b) to predominantly shear yielding (Fig. 6c) or shear yielding involving largely

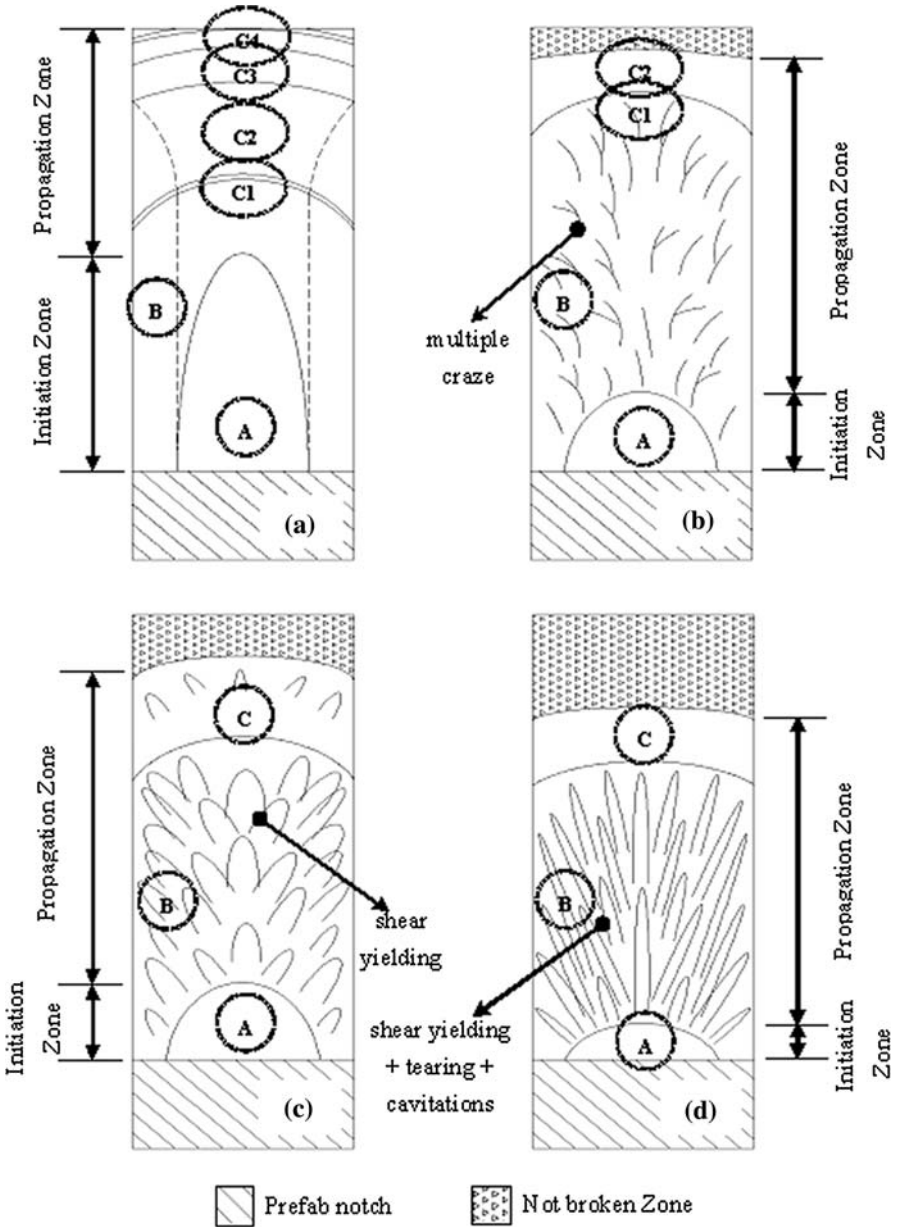

Fig. 6 Schematic of virgin PP, PP/POE and PP/POE/NA blend impact fracture surface morphologies. The crack propagation direction is upward

tearing and materials cavities (Fig. 6d), respectively. Expectedly, compared with virgin PP, the fractured surface becomes much rougher and the stick-slip stage moves further away from the root of notch. Furthermore, virgin PP presents large area of initiation zone and rapid crack-growth zone (brittle fracture mode). The presence of

POE decreases the initiation zone and induces shear lip zones at the edge of bar and less-ductile fracture zone at the later stage of fracture process. The initiation zone with brittle fracture feature becomes inconspicuous when NA (DMDBS or TMB-5) is present in the blend.

Crystalline structure transformation of PP/POE/β-NA during the impact process

A β to α phase transformation has often been discussed for the improved toughness of β nucleated materials during deformation. Especially, Tjong et al. [31] reported that β to α phase transformation is also present during impact test for β-PP. In this work, the possible crystalline structure transformation of TMB-5 nucleated samples were carefully detected by WAXD and DSC. Figure 7 shows DSC heating curves and the WAXD patterns of PP/β-NA and PP/POE/β-NA before and after impact test. For DSC measurements, before impact test, both PP/β-NA and PP/POE/β-NA show two weak endothermic peaks at the temperature of about 145 and 150 °C (Marked as β_1 and β_2), and these endothermic peaks are attributed to the melting of β-PP. After impact test, the endothermic peaks of β-PP become weaker, indicating the decrease of β-PP content. However, the stronger endothermic peak of α-PP after impact test suggests higher content of α-PP compared with the sample before impact test. So, it can be deduced that some β-PP changes into α-PP during the impact fracture process. The variations of diffraction intensity of β-PP (300) and α-PP (110) and the relative content of β-PP before and after impact test also prove the transformation of $\beta \rightarrow \alpha$ during the impact process, and the results are shown in Fig. 7b and Table 2, respectively. One should notice that POE has a role of preventing the transformation of $\beta \rightarrow \alpha$ during the impact process. This will be further studied in the next work.

Further analysis on toughening mechanism of PP/POE/NA

It is well known that the main mode of energy absorption during the impact process of elastomer toughened PP is shear yielding of matrix. The easier the shear yielding

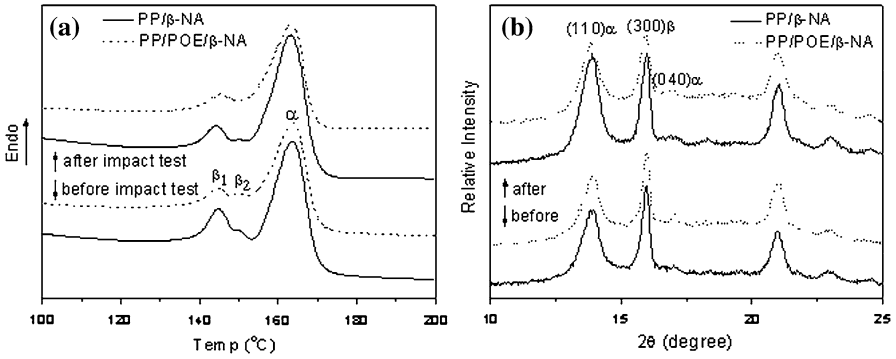

Fig. 7 The DSC heating curves (**a**) and WAXD profiles (**b**) of PP/β-NA and PP/POE/β-NA before and after impact test

Table 2 The variation of β-PP content before and after impact test

Sample	β-PP content (%)		Ratio of $\beta \rightarrow \alpha$ transformation (%)
	Before impact testing	After impact testing	
PP/β-NA	50.26	41.91	16.61
PP/POE/β-NA	47.21	41.89	11.27

of the matrix, the better the impact toughness of the blends is. Also, the shear yielding of the matrix is dependent on the matrix properties including spherulites size and crystalline morphology. As described above, both DMDBS and TMB-5 can influence the spherulites size and crystalline morphology significantly at the same processing conditions. The spherulites size decreases greatly and no spherulitic structure can be seen clearly. Considering the changes of impact toughness and fracture surface characteristic, we believe that tiny and uniform spherulites encouraged by NA must be the source of the improved toughness in PP/POE/NA blend. In general, the increased tie-molecular in the presence of NA in PP and its blends can improve spherulites boundaries [32]. Also, the tiny and uniform spherulites avoid the strong stress concentration at the interface of spherulites. In other words, the presence of NA in PP/POE enhances interaction among spherulites boundaries and decreases stress concentration at the spherulites boundaries. Therefore, during impact process, craze formation induced by POE particles tends to occur in the lamellae in large region and then shear yielding of PP matrix takes place largely, while the tendency of failure may be preferentially initiated at the spherulites boundaries for PP/POE binary blend due to the weaker interaction between spherulites boundaries compared to lamellae.

Especially, for PP/POE/β-NA blend, besides spherulites size, the presence of β-PP is a substantial origin for the significant enhancement in toughness due to the special spherulites structure. β-PP is a stacked, parallel arrangement of bundles of lamellae, whereas so-called "cross-hatched" arrangement of the lamellar crystal for α-PP [26]. The presence of the β-PP crystallites induces a higher continuity of the amorphous phase and more connecting bridges between individual crystallites than a material containing solely α-PP. Better structural continuity is macroscopically reflected as higher drawability and toughness [33]. During the impact process, not only the plastic glide in the lamellae induced by the stress around POE particles, but the tearing of amorphous chains in PP matrix becomes easier. Furthermore, the variation of β-PP relative content before and after impact test shows that POE has a role of preventing the transformation of $\beta \rightarrow \alpha$. More β-PP is maintained and participates in the plastic deformation or shear yielding, inducing higher energy absorption during the impact process.

Conclusion

In the present work, the impact fracture behaviors of virgin PP, PP/POE and PP/POE/NA have been investigated comparatively. The results show that POE induces

the fracture behavior changing from the typical brittle feature of virgin PP to less-ductile feature (multiple-craze formation) of PP/POE. Interestingly, PP/POE/NA shows apparent ductile characteristics with sever plastic deformation or shear yielding in large area. Especially for PP/POE/β-NA blend, besides the plastic deformation of matrix, large amounts of materials cavitations and second-crack re-initiation are observed in the impact-fractured surface, indicating the dramatic energy absorption. Our results also show the transformation of $\beta \rightarrow \alpha$ during the impact process for β-NA nucleated sample and the presence of POE prevents such transformation.

Acknowledgments We would like to express our sincere thanks to National Natural Science and Technology Foundation (No. 50403019) and Sichuan Youthful Science and Technology Foundation (07ZQ026-003) (P.R. China) for supporting this work.

References

1. Tam WY, Cheung T, Li RKY (1996) An investigation on the impact fracture characteristics of EPR toughened polypropylene. Polym Test 15:363–380
2. D'Orazio L, Mancarella C, Martuscelli E, Cecchin G, Corrieri R (1999) Isotactic polypropylene/ethylene-co-propylene blends: effects of the copolymer microstructure and content on rheology, morphology and properties of injection moulded samples. Polymer 40:2745–2757
3. Silva da ALN, Coutinho FMB (1996) Some properties of polymer blends based on EPDM/PP. Polym Test 15:45–52
4. Van der Wal A, Nijhof R, Gaymans RJ (1999) Polypropylene–rubber blends: 2. The effect of the rubber content on the deformation and impact behaviour. Polymer 40:6031–6044
5. Premphet K, Paecharoenchai W (2002) Polypropylene/metallocene ethylene–octene copolymer blends with a bimodal particle size distribution: mechanical properties and their controlling factors. J Appl Polym Sci 85:2412–2418
6. Borggreve RJM, Gaymans RJ, Schuijer J, Ingen Housz JF (1987) Brittle–tough transition in nylon–rubber blends: effect of rubber concentration and particle size. Polymer 28:1489–1496
7. Jiang W, An LJ, Jiang BZ (2001) Brittle–tough transition in elastomer toughening thermoplastics: effects of the elastomer stiffness. Polymer 42:4777–4780
8. Jiang W, Wang ZG, Liu CH, Liang HJ, Jiang BZ, Wang XH, Zhang HX (1997) Effect of γ-irradiation on brittle–tough transition of PBT/EPDM blends. Polymer 38:4275–4277
9. Jang BZ, Uhlmann DR, Vander Sande JB (1985) The rubber particle size dependence of crazing in polypropylene. Polym Eng Sci 25:643–651
10. Kim DS, Cho K, Kim JK, Park CE (1996) Effects of particle size and rubber content on fracture toughness in rubber-modified epoxies. Polym Eng Sci 36:755–768
11. Van der Wal A, Gaymans RJ (1999) Polypropylene–rubber blends: 5. Deformation mechanism during fracture. Polymer 40:6067–6075
12. Wang Y, Fu Q, Li QJ, Zhang G, Shen KZ, Wang YZ (2002) Ductile–brittle-transition phenomenon in polypropylene/ethylene–propylene–diene rubber blends obtained by dynamic packing injection molding: a new understanding of the rubber-toughening mechanism. J Polym Sci Part B Polym Phys 40:2086–2097
13. Wang Y, Zhang Q, Na B, Du RN, Fu Q, Shen KZ (2003) Dependence of impact strength on the fracture propagation direction in dynamic packing injection molded PP/EPDM blends. Polymer 44:4261–4271
14. Guerrica-Echevarría G, Eguiazábal JI, Nazábal J (2007) Influence of compatibilization on the mechanical behavior of poly(trimethylene terephthalate)/poly(ethylene–octene) blends. Eur Polym J 43:1027–1037
15. Bucknall CB, Smith RR (1965) Stress-whitening in high-impact polystyrenes. Polymer 6:437–446
16. Newman S, Strella S (1965) Stress–strain behavior of rubber-reinforced glassy polymers. J Appl Polym Sci 9:2297–2310

17. Jiang W, Yuan Q, An LJ, Jiang BZ (2002) Effect of cavitations on brittle–ductile transition of particle toughened thermoplastics. Polymer 43:1555–1558
18. Wu S (1985) Phase structure and adhesion in polymer blends: a criterion for rubber toughening. Polymer 26:1855–1863
19. Van der Wal A, Mulder JJ, Oderkerk J, Gaymans RJ (1998) Polypropylene–rubber blends: 1. The effect of the matrix properties on the impact behaviour. Polymer 39:6781–6787
20. Jiang W, Yu DH, Jiang BZ (2004) Brittle–ductile transition of particle toughened polymers: influence of the matrix properties. Polymer 45:6427–6430
21. Grein C, Plummer CJG, Kausch HH, Germain Y, Béguelin Ph (2003) Influence of β nucleation on the mechanical properties of isotactic polypropylene and rubber modified isotactic polypropylene. Polymer 43:3279–3293
22. Bai HW, Wang Y, Song B, Li YL, Liu L (2008) Effect of nucleating agent on the brittle–ductile transition behavior of polypropylene/ethylene–octene copolymer blends. J Polym Sci Part B Polym Phys 46:577–588
23. Bai HW, Wang Y, Song B, Han L (2008) Synergistic toughening effects of nucleating agent and ethylene–octene copolymer on polypropylene. J Appl Polym Sci 108:3270–3280
24. Fanegas N, Gómez MA, Jiménez I, Marco C, Garcia-Martínez JM, Ellis G (2008) Optimizing the balance between impact strength and stiffness in polypropylene/elastomer blends by incorporation of a nucleating agent. Polym Eng Sci 48:80–87
25. Turner-Jones A, Aizlewood JM, Beckett DR (1964) Crystalline forms of isotactic polypropylene. Makromol Chem 75:134–158
26. Henning S, Michler GH (2005) Micromechanical deformation mechanisms in polyolefins: influence of polymorphism and molecular weight. In: Michler GH, Baltá-Calleja FJ (eds) Mechanical properties of polymers based on nanostructure and morphology. Taylor & Francis, Boca Raton, pp 245–278
27. Misra RDK, Hadal R, Duncan SJ (2004) Surface damage behavior during scratch deformation of mineral reinforced polymer composites. Acta Mater 52:4363–4376
28. Misra RDK, Nathani H, Dasari A, Wanjale SD, Jog JP (2004) The determining role of clay particles on mechanically induced surface damage and associated stress whitening in polybutene–clay nanocomposites. Mater Sci Eng A 386:175–185
29. Speroni F, Castoldi E, Fabbri C, Casiraghi T (1989) Mechanisms of energy dissipation during impact in toughened polyamides: a SEM analysis. J Mater Sci 24:2165–2176
30. Muratoğlu OK, Argon AS, Cohen RE, Weinberg M (1995) Microstructural processes of fracture of rubber-modified polyamides. Polymer 36:4771–4786
31. Tjong SC, Shen JS, Li RKY (1996) Morphological behaviour and instrumented dart impact properties of β-crystalline-phase polypropylene. Polymer 37:2309–2316
32. Avella M, Dell'Erba R, Martuscelli E, Ragosta G (1993) Influence of molecular mass, thermal treatment and nucleating agent on structure and fracture toughness of isotactic polypropylene. Polymer 34:2951–2960
33. Zhang PY, Liu XX, Li YQ (2006) Influence of β-nucleating agent on the mechanics and crystallization characteristics of polypropylene. Mater Sci Eng A 434:310–313